Imperfect homoclinic bifurcations

Paul Glendinning
Department of Mathematics, UMIST, P.O. Box 88, Manchester M60 1QD, United Kingdom

Jan Abshagen and Tom Mullin
Manchester Center for Nonlinear Dynamics, University of Manchester, Oxford Road, Manchester M13 9PL, United Kingdom

(Received 26 March 2001; published 21 August 2001)

Experimental observations of an almost symmetric electronic circuit show complicated sequences of bifurcations. These results are discussed in the light of a theory of imperfect global bifurcations. It is shown that much of the dynamics observed in the circuit can be understood by reference to imperfect homoclinic bifurcations without constructing an explicit mathematical model of the system.

DOI: 10.1103/PhysRevE.64.036208 PACS number(s): 05.45.Gg, 02.30.Oz

I. INTRODUCTION

The role of symmetries in determining the behavior of nonlinear physical systems can be crucial. Reflection (or $\mathbf{Z}_2$) symmetry is relevant to a wide range of experiments, and in such a system a pair of stable solutions may be created by a supercritical pitchfork bifurcation as a parameter is varied. These new states break the original symmetry, but are symmetric images of each other. Of course, perfect symmetry is never achievable in any physical system. So, in practice, the bifurcation may become disconnected having one branch that varies monotonically with the parameter and a second one that arises by a saddle-node bifurcation. This is most easily modeled by adding an imperfection term as a constant in the model normal form and this appears to work well in describing the local bifurcation structure. However, a physical system will typically contain many sources for this imperfection and some of them may be high dimensional in nature. Therefore, it is reasonable to ask whether a model with a single imperfection term provides a good representation of the system far from the bifurcation point. Specifically, we are interested here in the effects of this local modeling on the global dynamics that result from homoclinic bifurcations.

Our investigation is concerned with a class of global bifurcations involving homoclinic orbits, i.e., orbits that tend to a stationary point of the model flow in both forward and backward time. Typically, the existence of a homoclinic orbit is not a persistent property of a differential equation, but they occur on lines in two-parameter families (technically, they are codimension-1 bifurcations). In the absence of symmetry, the net effect of such bifurcations is to create or destroy a periodic orbit, whose period tends to infinity at the bifurcation point. This may happen in one of two ways: one sided or two sided. In the one-sided case, the orbit approaches the bifurcation point from one side of the bifurcation point as its period tends to infinity. In the two-sided case, such as the Shil'nikov case [1], the locus of the orbit in parameter space oscillates about the bifurcation value creating the so-called ''Shil'nikov wiggle'' as the period of the orbit tends to infinity. Moreover, there are period-doubling and reverse period-doubling bifurcations of the orbit together with more complicated homoclinic bifurcations. This sequence of events has been reported previously [2] in an experimental and theoretical study of a modified van der Pol oscillator, and in a wide variety of other experiments including Taylor-Couette flows [3,4], optics [5,6], chemical oscillators [7,8], and liquid crystal flows [9].

In the presence of simple symmetries, homoclinic bifurcations may involve two or more homoclinic orbits. In the simplest cases the net effect is to destroy a pair of periodic orbits, which are the images of each other under the symmetry and create a single symmetric branch of periodic orbits. These symmetric periodic orbits cannot undergo period-doubling. So in the two-sided case, the period-doubling and reverse period-doubling bifurcations on branches of the symmetric orbit are replaced by an initial symmetry-breaking (or reverse symmetry-breaking) bifurcation. The asymmetric orbits created in this way may, of course, be involved in period-doubling bifurcations. This distinction will be useful in the interpretation of the bifurcations observed below.

Whilst the effect of small symmetry-breaking terms on the bifurcations of stationary solutions has a long history (the imperfection theory of Golubitsky and Schaeffer [10–12]) there appears to have been no systematic attempt to describe the equivalent modifications of global bifurcations (see [13,14] for a special case). Our aim here is to consider the simplest possible case and to compare the predictions with the results of a complimentary experiment. Although we do not take the precise details of the symmetry-breaking terms into account, qualitative agreement with the experimental results is found.

We reconsider the experimental electronic oscillator [2] that exhibits a variety of almost symmetric global bifurcations and show how many features observed in the experiments may be explained by reinterpreting some results on codimension-2 homoclinic bifurcations so as to obtain a general imperfection theory for homoclinic bifurcations. These results necessarily involve nonstationary solutions, and so are likely to be applicable and observable in many more interesting situations.

The experiments were carried out using a van der Pol oscillator. The bifurcation structure of this system has been investigated in detail previously [2] but with the implicit assumption of symmetry. It is the aim of the present study to investigate the global dynamics of the circuit and relate the

observations to modern ideas on gluing bifurcations where the mathematical abstraction of perfect symmetry is relaxed.

II. EXPERIMENT I

A. The electronic oscillator

The experimental study was performed using a van der Pol oscillator circuit, the details of which are given in Healey *et al.* [2]. It comprises an autonomous LCR oscillator with two nonlinear conductances in the feedback circuit. Precise variation of the two parameters that control the behavior of the system was provided by switchable decades resistance boxes. This means determination of the bifurcation structure to a relative accuracy of better than 0.1% was possible. The two parameters are denoted by α_1,β_1 and they are nondimensionalized forms of the resistances R_1,R_2 that control the nonlinear elements. Details of the nondimensionalization are given in Healey *et al.* [2].

The principle set of observations were made using an oscilloscope. Steady bifurcations were observed as changes in the level of the dc output. On the other hand dynamical states were best monitored as Lissajous figures formed from a combination of signals measured over the nonlinear elements. In this way, limit cycles, period-doubling sequences, chaos etc. were readily displayed. Time series were also recorded and stored on a computer via a 12-bit A/D for further processing. This included phase portrait analysis using the method of delay coordinates.

The inductor used in the present circuit is 1.5269H compared with 1.78H used by Healey *et al.* [2]. This causes a shift of the bifurcation points relative to those previously reported, though the bifurcation structure remains qualitatively the same. The imperfections in the circuit are tiny and the resulting local bifurcation diagrams are very close to those we would expect from a perfect system. Although the symmetry-breaking term arises from a variety of sources, we will refer to them throughout as a single imperfection.

B. Bifurcation set

The stability diagram for the electronic circuit is shown in Fig. 1. The overall structure shows lines of steady and dynamic bifurcations, all meeting at the top right hand corner of the figure that is a codimension-2 point. The dynamic bifurcations (Hopf and homoclinic) are pairs of lines superposed and separated by the imperfections in the circuit. This effect is very small and cannot be resolved on the scale of the figure but, as we will show below, it has a significant effect on the global dynamics.

In the parameter range of interest, a perfectly symmetric system would have a trivial 0 V fixed point that would lose stability to a pair of nonzero dc states at a supercritical pitchfork bifurcation. As expected, in the experiment we see that this bifurcation is disconnected to form a continuously connected state and a separate solution branch that is terminated at its lower end by a saddle-node bifurcation denoted by SN in Fig. 1. The stable nontrivial asymmetric dc states both become time dependent via Hopf bifurcations; one on each branch. The imperfection in the circuit is very small, so the

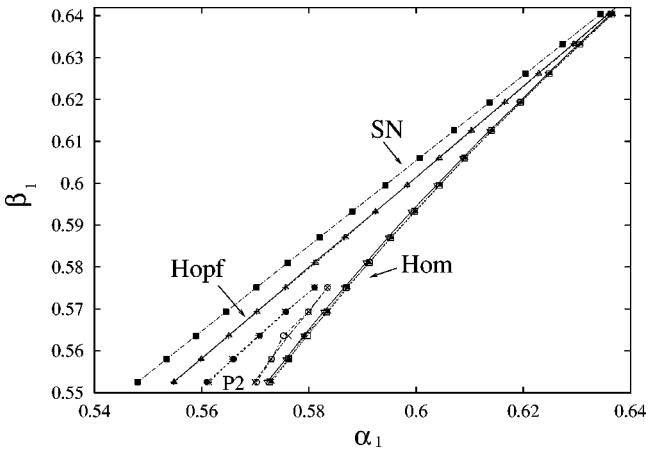

FIG. 1. Experimental bifurcation set in the α_1,β_1 plane. SN denotes the path of saddle-node bifurcations, ''Hopf'' the Hopf bifurcations to simple oscillations, and ''Hom'' the gluing bifurcations. The parameter region denoted by ''$P2$'' is where forward and reverse period doubling is observed on the asymmetric orbits.

loci of these bifurcations almost coincide and are marked ''Hopf'' in Fig. 1. The two asymmetric limit cycles that arise at the Hopf bifurcations appear to glue together leading to a large symmetric periodic orbit. This transition is denoted by the line marked ''Hom'' in Fig. 1 and will be discussed in detail below. This symmetric limit cycle undergoes different types of bifurcation including symmetry breaking and period doubling and may also become chaotic. Finally, within the oscillatory regime forward and reverse period-doubling sequences have been observed and these can be related to the Shil'nikov wiggle as shown by Healey *et al.* [2]. The boundaries of this region are denoted by $P2$ in Fig. 1.

C. Imperfect gluing bifurcation

We first examine the influence of the imperfection on the gluing bifurcation that occurs when the two asymmetric limit cycles join without the presence of complicated dynamics. We chose β_1 sufficiently large ($\beta_1 \geqslant 0.59$ approximately) and α_1 close to β_1 so that the chaos that arises from period-doubling sequences on a Shil'nikov wiggle is avoided and the dynamics is almost planar. We present a ''typical'' set of results for the orbit structure of the oscillator in this regime in Figs. 2 and 3 that were taken at $\beta_1=0.6000$. Figure 2 shows the period of the various simple orbits observed as a function of the parameter α_1, and Fig. 3 shows the form of the corresponding orbits—the two small asymmetric orbits are labeled by ''1'' and ''0,'' respectively, and the large amplitude orbit is labeled by ''10,'' for reasons that will be explained below.

If the electronic oscillator were symmetric then the development of the orbits shown in Fig. 3 for $\alpha_1=0.6041$ would have a simple explanation in terms of gluing bifurcations [15]: two periodic orbits that are the symmetric image of each other approach a stationary point and are ''glued together'' to form single symmetric orbit with code ''10.'' At the bifurcation the two smaller periodic orbits touch at the stationary point, i.e., they are no longer periodic (their period has diverged to infinity) and they form two homoclinic or-

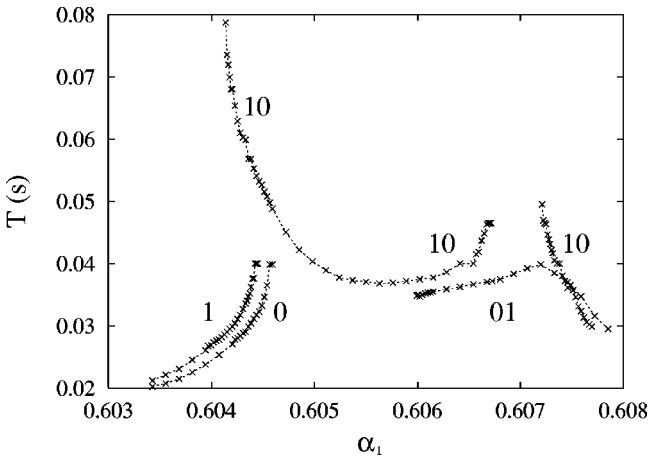

FIG. 2. Oscillation period of different periodic orbits at $\beta_1 = 0.6000$ plotted as a function of α_1. "1" and "0" denote the orbits on the asymmetric branches and "10", "01" are the glued orbits.

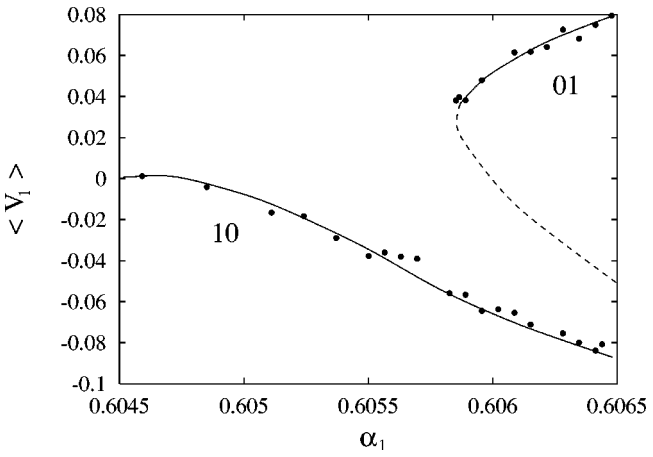

FIG. 4. Bifurcation diagram of symmetry-breaking bifurcation of periodic orbits at $\beta_1 = 0.6000$. The mean of V_1 over 5000 data points is plotted.

bits, biasymptotic to the stationary point.

As is clear from Fig. 2, and as should be expected of a real physical system, the oscillator is not perfectly symmetric. Hence it is not surprising that the pair of homoclinic orbits that exist at a single parameter value in the symmetric system seem to occur at different parameter values in the oscillator. The results shown in Fig. 2 also suggest that there is a third homoclinic bifurcation—the bifurcation that creates the large amplitude "10" periodic orbit.

It can be seen in Fig. 2 that the period of both the small asymmetric orbits "1" and "0" increases as α_1 increases and they finally lose stability and jump to the "10" orbit at $\alpha_1 \approx 0.6045$, i.e., where the graphs of the variation of period are almost vertical. Moreover, the "0" orbit remains stable for slightly higher values of α_1 than the "1" orbit, emphasizing that the two orbits are not the images of each other under the symmetry. It should be noted that the "1" orbit results from a Hopf bifurcation on the monotonic branch of the disconnected pitchfork bifurcation. Therefore it loses stability before the "0" orbit. This is precisely what is predicted by the addition of a constant term to the normal form. The orbits shown in Fig. 3 all coexist at $\alpha_1 = 0.6041$ and are typical examples of the limit cycles involved in this gluing bifurcation. The fact that they can all coexist explains why hysteresis can be observed in the experiments.

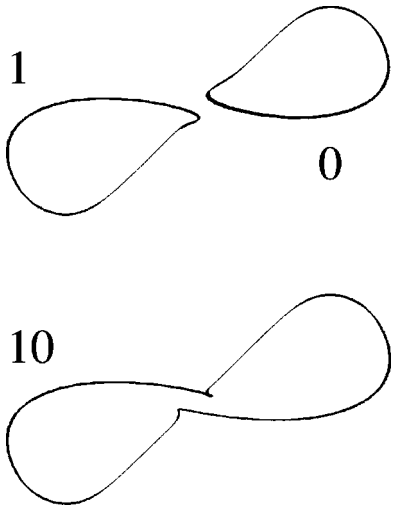

FIG. 3. Phase portraits of coexisiting asymmetric (1,0) and symmetric (10) periodic orbits at $\alpha_1 = 0.6041$ and $\beta_1 = 0.6000$.

There are three features in Fig. 2 that we will seek to explain theoretically in the following section: the break up of the gluing bifurcation, hysteresis, and also the extra bifurcations evident at larger values of α_1. Before describing the theory we shall look at this latter sequence of bifurcations in more detail.

D. Symmetry-breaking bifurcation of large periodic orbit

It is known that symmetric systems cannot undergo period-doubling sequences directly [16] but must first break their symmetry. Hence, we would expect the large symmetric orbit formed by the gluing of the two asymmetric ones to undergo a symmetry-breaking bifurcation, as predicted for the symmetric Shil'nikov wiggle [17]. As expected, this bifurcation is disconnected in the experiment and has been observed at $\beta_1 = 0.6000$ with α_1 increasing from 0.6059. The bifurcation was detected by measuring the mean voltage averaged over 150 periods of the oscillation and plotting this as a function of α_1. The resulting bifurcation diagram is shown in Fig. 4 where we see that it has the form of a disconnected pitchfork. This diagram explains the creation of the orbit labeled "01" in Fig. 2. Note that the original "10" orbit has a larger period but smaller $\langle V_1 \rangle$ than the newly created "01" orbit. Hence, the branches in Figs. 2 and 4 are apparently reversed. Two typical asymmetric orbits on respective branches are shown in Fig. 5 for $(\alpha_1, \beta_1) = (0.6067, 0.6000)$. It was observed that the period of "10" orbit (cf Fig. 2) on the connected branch varied rapidly for $\alpha_1 > 0.6065$ and then loses stability. However, the period of the "01" orbit is virtually constant over this range. At higher α_1 values the periods of both orbits decreased. Each orbit underwent period-doubling sequences to chaos for α_1 values

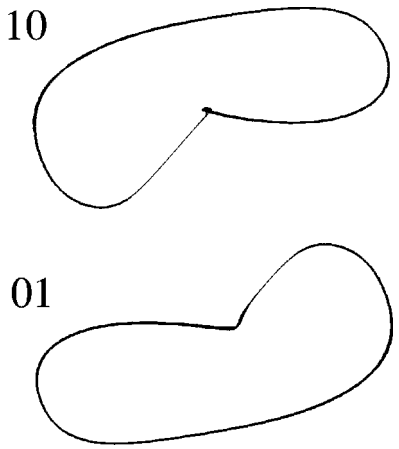

FIG. 5. Phase space portrait of coexisiting "large" periodic orbits 10 and 01 at $\beta_1=0.6000$ and $\alpha_1=0.6067$.

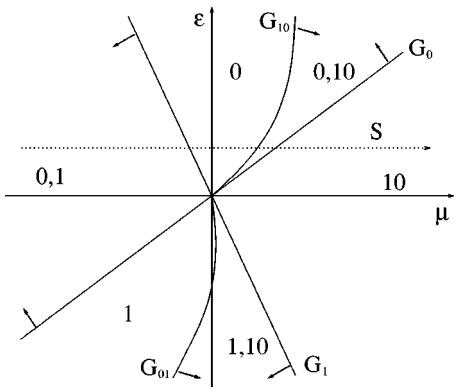

FIG. 6. The two parameter plane for the imperfect gluing bifurcation in the planar case. A one-parameter family of (imperfect) systems S is indicated by a curve through the plane close to $\epsilon=0$. The arrows indicate the direction in which orbits are created.

greater than the range displayed in Fig. 2. The extra complications of period doubling and instability are topics for future research.

III. THEORY

It is natural to think of the bifurcations observed in the system in terms of two parameters. One of these, say μ, is the parameter of the (fictional) symmetric system that has a gluing bifurcation as described in Sec. II C. The second parameter, say ϵ, is a measure of how far the oscillator is from being perfectly symmetric, i.e. it is some measure of imperfection with $\epsilon=0$ corresponding to the perfectly symmetric system. Just as the standard imperfection theory for the bifurcations of stationary points [12] allows one to describe the effect of asymmetry in terms of μ and ϵ, our aim here is to give an analogous description for general global bifurcations. We note that this is in the spirit of the work of Glendinning [14] and Cox [13] for the particular case of Lorenz-like bifurcations.

A. The basic picture

Suppose that $(\mu,\epsilon)=(0,0)$ denotes the point in parameter space at which there are two symmetrically related homoclinic orbits. Consider either one of these orbits. Since the existence of homoclinic orbits is codimension 1, there will be a curve in parameter space through (0,0) on which systems have a homoclinic orbit that is a continuation of the given orbit. Thus, for typical two-parameter families of systems, there will be two curves of homoclinic orbits in parameter space, say G_0 and G_1, which intersect at the origin and that do not intersect the line $\epsilon=0$ again locally. The curve G_0 (respectively, G_1) is the locus of a homoclinic bifurcation that creates or destroys the periodic orbit with code 0 (respectively, 1). The one-parameter families of nearly symmetric systems such as the example considered in the preceding section would then correspond to some curve in this two-parameter space that has, for example, $\epsilon>0$ and that passes close to $(\mu,\epsilon)=(0,0)$. Such a curve will intersect both G_0 and G_1, but at different parameter values, so there will be two simple homoclinic bifurcations at nearby parameter values on such a path.

The intersection of the loci of two homoclinic bifurcations (each to the same stationary point) is a codimension-2 phenomenon that has been studied by a number of authors [15,18–24]. The most important feature that all these bifurcations have in common is that at least two other curves of homoclinic orbits emanate from the intersection of G_0 and G_1, one in $\epsilon>0$ labeled G_{10}, and the other in $\epsilon<0$ labeled G_{01}. The labeling describes the order (in time) that the orbit passes through neighborhoods of the basic homoclinic orbits. These homoclinic orbits are precisely the bifurcations needed to destroy or create (asymmetric) periodic orbits with code "10" or "01." Thus a typical path close to $\epsilon=0$ will intersect G_0, G_1 and one of the curves G_{01} or G_{10}. This explains the third homoclinic bifurcation observed in Fig. 2. Roughly speaking, the difference between orbits created by paths crossing G_{10} and those created by crossing G_{01} is the difference between the orbits shown in Fig. 5.

The details of the two-parameter bifurcation plane close to the intersection of G_0 and G_1 depends upon the nature of the stationary point, the configuration of the homoclinic orbits and a measure of the amount of twisting of solutions about these orbits. The nature of the stationary point is determined by the eigenvalues of the Jacobian matrix of the flow that are closest to the imaginary axis. If, up to complex conjugation, these are λ_1 and λ_2 with $\mathrm{Re}\,\lambda_1<0<\mathrm{Re}\,\lambda_2$ then the *saddle index* δ defined by

$$\delta=-\mathrm{Re}\,\lambda_1/\mathrm{Re}\,\lambda_2 \tag{1}$$

plays an important role. The two-parameter space near the intersection of G_0 and G_1 in the planar case is shown in Fig. 6 (λ_1 and λ_2 are real), where the symmetry is a point symmetry about the stationary point and the direction of time may be chosen so that $\delta>1$. Each simple homoclinic bifurcation creates a periodic orbit in the direction indicated by arrow on the bifurcation curve. The parameter plane is divided into six regions by the curves of bifurcations, and the periodic orbits (from the local theory) that exist in each re-

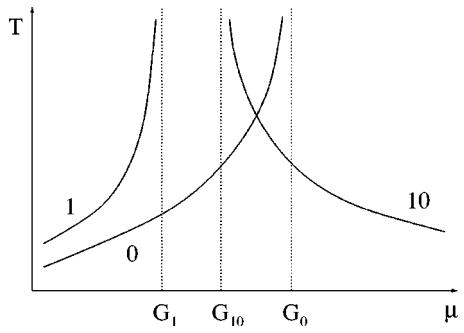

FIG. 7. Bifurcation diagram (period against parameter) on the one-parameter path *S* of Fig. 6.

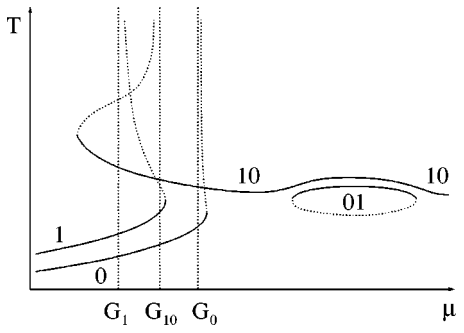

FIG. 8. Bifurcation diagram (period against parameter) of the modified global bifurcation as suggested by Fig. 2.

gion are indicated by their codes. The bifurcations observed on the one-parameter path *S* in Fig. 6 are shown in Fig. 7, which is the more conventional representation.

B. Relationship with the experiment

The curves sketched in Fig. 7 are in reasonably good agreement with the experimental ones in Fig. 2 except for the extra complications at larger parameter values described in Sec. II D. Also the fact, mentioned at the end of Sec. II C, that all three of the orbits labeled "0," "1," and "10" coexist for some values of α_1. However, even these aspects can be incorporated into our picture of imperfect global bifurcations. For smaller values of β_1 Shil'nikov wiggles are observed, suggesting that $\delta<1$ (and λ_1 is complex) in this parameter regime. In this case, as earlier, there may be symmetry-breaking and reverse symmetry-breaking bifurcations of the symmetric orbit (in the perfectly symmetric system) [17]. The bifurcations observed in Fig. 2 and described in more detail in Fig. 4 are not in the asymptotic region of applicability of the homoclinic theory (large period, close to homoclinic bifurcation) and so we invoke an extra pair of assumptions on the underlying symmetric system for our model: that there is a symmetry-breaking and reverse symmetry-breaking bifurcation on the symmetric orbit and that $\delta<1$.

If $\delta<1$ then the curves of homoclinic bifurcations are essentially as in Fig. 6 but the direction of the bifurcations is reversed (more precisely, the diagram is reflected about the ϵ axis) and the orbits created are saddles (rather than stable, as would be the case if $\delta>1$). This now suggests the new interpretation of Fig. 2 that is shown in Fig. 8. The major new feature is that since the orbits are created in the opposite direction to the case with $\delta>1$ in Fig. 6 and are unstable, the points at which the orbits cannot be followed further ($\alpha_1=0.6041$ for the "10" orbit and $\alpha_1=0.6025$ for the "0" and "1" orbits in Fig. 2) are now assumed to be saddle-node bifurcations. There are a number of possible interpretations for the disconnected symmetry-breaking bifurcations, and one of these is shown in Fig. 8, although we make no claim that it is the most likely. Note that the new arrangement of the homoclinic bifurcations does provide a region of parameters where the orbits "0," "1," and "10," coexist and are stable, as seen in the experiment.

The important feature of the analysis above is that two assumptions about the underlying mathematical model are sufficient to explain the orbits observed in the experiment. It is worth emphasizing that this can be done *without* constructing the model equations explicitly, simply by suggesting that any model equation must have various dynamical features.

C. Other cases

In the literature, codimension-2 global bifurcations are generally described with G_0 and G_1 (the loci of the simple homoclinic bifurcations) as the coordinate axes of the bifurcation analysis. In this case the symmetric system may be assumed to lie on the diagonal of the parameter space. It is, however, important to bear in mind that in models of physical systems the curves G_0 and G_1 intersect with a very small angle of intersection, whereas the standard analysis depicts the intersection to be at right angles. Provided the intersection is transversal the analysis holds, although it does mean that the true picture for the asymmetric perturbation is a very skewed version of the standard pictures.

All the relevant types of bifurcation we have considered have a basic feature in common. As the bifurcation parameter μ is varied, a (more or less complicated) sequence of bifurcation is observed with the net effect that a pair of periodic orbits (those we have labeled "0" and "1") is destroyed, and a single large periodic orbit is created. The precise details of the bifurcations depend on the system, but it is still possible to make a number of general statements.

1. The one-sided case

If the direction of time can be chosen so that λ_2 is real and $\delta>1$ [cf. Eq. (1)] then the codimension-1 bifurcations on G_0 and G_1 are one sided and fairly general statements about the bifurcations involved in the range of validity of the rigorous argument: large period and parameters close to the intersection of G_0 and G_1 are possible [22]. First, there are at most two periodic orbits, and second, any periodic orbit has a very particular description in terms of the symbols "0" and "1" introduced above. Technically, the sequences are rotation compatible sequences [22], but in practice a simple consequence is that periodic orbits have codes of the form

$$01^{n_1}01^{n_2}01^{n_3}01^{n_4}01^{n_5}\ldots, \tag{2}$$

where for all i, $n_i\in\{m,m+1\}$ for some $m>0$ (or the same with the roles of 0 and 1 exchanged). Moreover, the limit ρ

of the number of 1*s* in the sequence to the length of the sequence exists and is called the rotation number of the orbit. In one case (the so-called stable orientable Lorenz-like case, see [21]), there is an infinite set of bifurcations along a typical path and at any one parameter after crossing the first bifurcation curve, there is at most one periodic orbit. Moreover, the rotation number varies continuously along the bifurcation path, implying the existence of parameter values with nonperiodic (but nonchaotic) attractors.

If λ_1 is complex then the range of bifurcations is more complicated and depends on the precise path taken through the parameter space. Here there are regions of coexistence of certain periodic orbits—those whose rotation numbers p_1/q_1 and p_2/q_2 are Farey neighbors, i.e., $|p_1q_2-q_1p_2|=1$—but typical curves in parameter space do not intersect most of these regions. A more complete list of the possibilities can be found in Refs. [17,18,21].

All the bifurcations of the rigorous analysis involve one-sided global bifurcations, and there are no local bifurcations on the branches of each periodic orbit. If these occur it is necessary to appeal to effects outside the rigorous region of validity of the mathematical results—this is made much easier by an understanding of the two-sided bifurcations.

2. The two-sided case: Shil'nikov's wiggle

The symmetric bifurcation diagram of the Shil'nikov case (λ_1 complex, λ_2 real and $\delta<1$) is given in Ref. [17]. The locus of the pair of orbits (''0'' and ''1'') in parameter-period space oscillates as the period increases to infinity, with period-doubling and reverse period-doubling bifurcations on every other branch. The symmetric orbit oscillates in a similar way, but with symmetry-breaking bifurcations on every other branch. Breaking the symmetry of the system will have two effects—the global bifurcations that coincide in the symmetric system will be split apart and the symmetry-breaking bifurcations will typically become disconnected as described above. In the two-parameter diagram close to the intersection of G_0 and G_1, curves of more complicated bifurcations (G_{01} and G_{10}) oscillate rapidly and intersect each other (there are infinitely many other curves of homoclinic bifurcations to complicate matters further). For a typical asymmetric path there will be a single intersection with G_0 and G_1, but potentially several intersections with G_{10} and G_{01}. The orbits created in the bifurcations involving G_0 and G_1 will lie on the usual Shil'nikov wiggle in the parameter-period plane as observed experimentally (see Fig. 9). The symmetric orbit, ''10,'' can also be followed experimentally (see Fig. 10); there are multiple intersections of the parameter path with G_{10}, i.e., extra bifurcations that create and destroy the orbits labeled ''10*.'' Between the conjectured intersection of the parameter path with G_0 and G_{10} it is possible to observe a stable orbit with code ''100.'' Such an orbit can be created from homoclinic orbits obtained from the gluing of the orbits ''10'' and ''0.'' These bifurcations are expected due to the intersection of G_0 and G_{10} in the two-parameter analysis (cf. the $\delta>1$ case in [22]) that create extra curves of homoclinic orbits G_{010} and G_{100}.

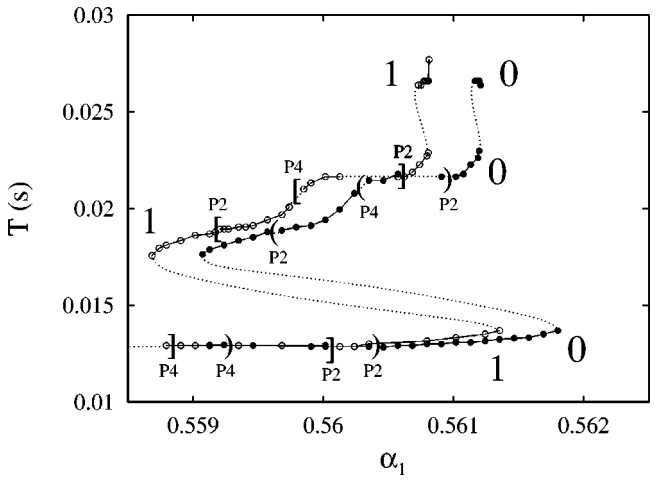

FIG. 9. Coexisiting Shil'nikov wiggle at $\beta=0.5317$. The branch noted with [ ] corresponds to the ''1'' and with ( ) to the ''0'' orbit respectively.

IV. EXPERIMENT II

The gluing process in the non-planar region of parameter space involves complicated orbits that evolve on a Shil'nikov wiggle. A pair of these wiggles are shown in Fig. 9 where the period is plotted as a function of α_1 at fixed $\beta_1=0.5317$. Here the period of the orbit approaches infinity through a sequence of folds where alternate branches are unstable and indicated by dashed schematic lines in the figure. The stable solutions undergo forward and reverse period-doubling sequences on the first two folds whereas the highest period orbits only exist over a tiny range of the parameter. In a perfectly symmetric system these two wiggles would overlap completely. The effect of the imperfection in the circuit is to displace the two curves from one another.

A Shil'nikov wiggle has also been observed on the symmetric orbit and the results are shown in Fig. 10. There we can see three levels of the wiggle with period-doubling sequences. The ''10'' orbits in this case were asymmetric but

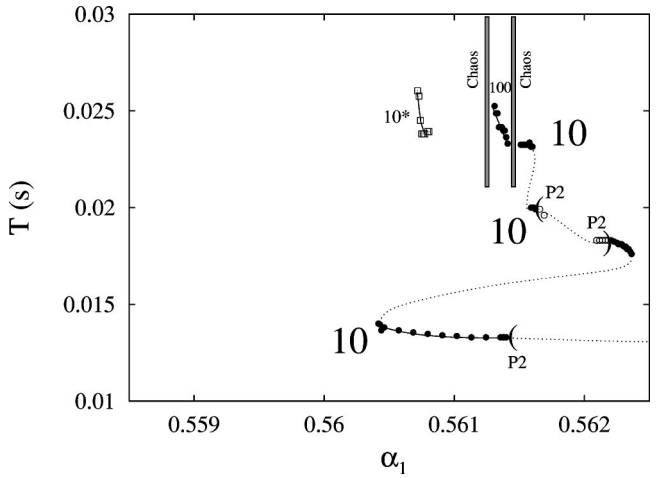

FIG. 10. Shil'nikov wiggle and gluing process of the ''10'' orbit at $\beta=0.5317$. The period of the ''10'' orbits and the ''100'' orbit is rescaled by 2 and 3, respectively.

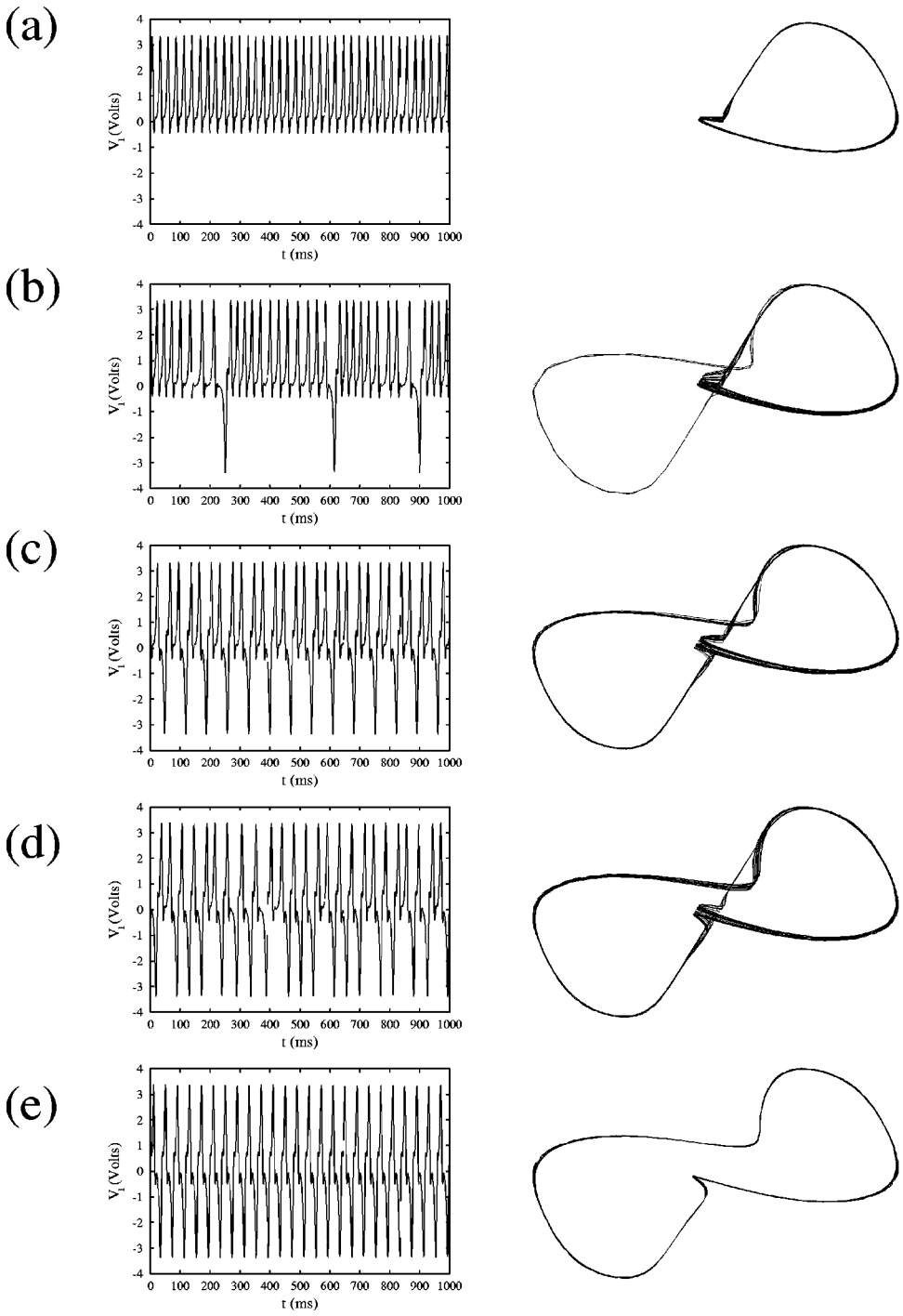

FIG. 11. Time series and phase portraits of different dynamical states involved in imperfect gluing bifurcation at $\beta = 0.5317$. (a) Periodic orbit ''0'' on asymmetric branch at $\alpha_1 = 0.561\,19$, (b) chaos at $\alpha_1 = 0.561\,25$, (c) period-3 orbit ''100'' at $\alpha_1 = 0.561\,36$, (d) chaos at $\alpha_1 = 0.561\,46$, (e) symmetric periodic orbit ''10'' at $\alpha_1 = 0.561\,52$.

we were unable to find the mirror image pairs of solutions in this case. We were, however, able to observe them at smaller values of β_1. The gluing process takes place on the third level with intervening sequences of chaos and a stable ''100'' orbit; as expected from the discussion at the end of Sec. III C. Note, we also observed the ''10*'' that is an integral part of the gluing process as discussed in Sec. III C above. A set of time series and phase portraits are displayed in Fig. 11. The ''0'' orbit on the disconnected branch glues to the ''10'' large scale orbit via two chaotic phases with an intermediate period-3 ''100'' sequence.

V. CONCLUSION

Although symmetric equations are frequently used to model almost symmetric systems, we have shown that a more careful examination of experiments can reveal features that do not appear in the symmetric models. In particular, we have focused here on global bifurcations that involve periodic states of the system, and we have shown how a number of complicated bifurcation diagrams observed in the experiments can be interpreted by appealing to a theory of imperfect homoclinic bifurcations.

A standard approach to the modeling of physical phenom-

ena is to construct a mathematical model of the experiment, and use this to either predict or explain features of the experiment. This entails both the construction of the model and the analysis of the model constructed. It is noticeable that in the approach taken here we have appealed to properties of a model *without* having to either construct or analyze the model. We have simply argued that any mathematical model of the experiments must have certain features, and that these features lead to certain conclusions by the application of global bifurcation theory. Clearly, a more precise description of the symmetry-breaking terms would be needed to make the correspondence between the model, theory, and experimental results quantitative rather than qualitative. This is a worthwhile project, but not one we have attempted here.

Bifurcation diagrams consistent with those of Sec. III have now been observed in more physically interesting systems. Abshagen *et al.* [25] has found bifurcation diagrams with a striking similarity to Fig. 6 in experimental data from fluid flow. We believe that the approach taken here will find application in a broad variety of experiments in which symmetry, or rather, almost symmetry, plays a role.

[1] P. Glendinning, *Stability, Instability and Chaos* (Cambridge University Press, Cambridge, 1994).

[2] J. J. Healey, D. S. Broomhead, K. A. Cliffe, R. Jones, and T. Mullin, Physica D **48**, 322 (1991).

[3] T. Mullin and T. J. Price, Nature (London) **340**, 294 (1989).

[4] J. von Stamm, U. Gerdts, T. Buzug, and G. Pfister, Phys. Rev. E **54**, 4938 (1996).

[5] E. Allaria, F. T. Arecchi, A. Di Garbo, and R. Meucci, Phys. Rev. Lett. **86**, 791 (2001).

[6] R. Herrero, R. Pons, J. Farjas, F. Pi, and G. Orriols, Phys. Rev. E **53**, 5627 (1996).

[7] M. J. B. Hauser and L. F. Olsen, J. Chem. Soc., Faraday Trans. **92**, 2857 (1996).

[8] A. Arnéodo, F. Argoul, J. Elezgaray, and P. Richetti, Physica D **62**, 134 (1993).

[9] T. Peacock and T. Mullin, J. Fluid Mech. **432**, 369 (2001).

[10] M. Golubitsky and D. Schaeffer, Commun. Pure Appl. Math. **32**, 21 (1979).

[11] M. Golubitsky and D. Schaeffer, Commun. Math. Phys. **67**, 205 (1979).

[12] D. Schaeffer, in *Dynamical Systems and Turbulence*, edited by D.A. Rand and L.-S. Young (Springer, Berlin, 1981).

[13] S. M. Cox, J. Fluid Mech. **227**, 1 (1991).

[14] P. Glendinning, Dyn. Stab. Syst. **2**, 43 (1987).

[15] P. Coullet, J.-M. Gambaudo, and C. Tresser, C. R. Acad. Sci., Ser. I: Math. **299**, 253 (1984).

[16] J. W. Swift and K. Wiesenfeld, Phys. Rev. Lett. **52**, 705 (1984).

[17] P. Glendinning, Phys. Lett. A **103**, 163 (1984).

[18] J.-M. Gambaudo, Thèse d'Etat, Université de Nice, 1987.

[19] J.-M. Gambaudo, P. Glendinning, and C. Tresser, C. R. Acad. Sci., Ser. I: Math **300**, 311 (1984).

[20] J.-M. Gambaudo, P. Glendinning, and C. Tresser, J. Phys. (France) Lett. **46**, L653 (1985).

[21] J.-M. Gambaudo, P. Glendinning, and C. Tresser, in *Instabilities and Nonequilibrium Structures*, edited by E. Tirapegui and D. Villarroel (D. Reidel, Dordrecht, 1987).

[22] J.-M. Gambaudo, P. Glendinning, and C. Tresser, Nonlinearity **1**, 203 (1988).

[23] D. V. Lyubinov, A. S. Pikovsky, and M. A. Zaks, Sov. Sci. Rev. C. Math. Phys. **8**, 221 (1989).

[24] D. V. Turaev and L. P. Shil'nikov, Dokl. Akad. Nauk SSSR **290**, 1301 (1986) [Sov. Math. Dokl. **34**, 397 (1987)].

[25] J. Abshagen, G. Pfister, and T. Mullin (unpublished).